Freely Propagating Trench Waves on a Beta-Plane

ANDREW J. WILLMOTT AND ARLENE A. BIRD

Department of Oceanography, Naval Postgraduate School, Monterey, CA 93940

(Manuscript received 12 November 1982, in final form 29 May 1983)

ABSTRACT

The dispersion relation is derived for trapped freely propagating barotropic long trench waves on a midlatitude β-plane. It is found that a critical wavenumber k_c, which depends on trench orientation and wave frequency, partitions the behavior of each mode. Leaky modes occur when the wavenumber k of a particular mode satisfies $k < k_c$, in which case the mode takes the form of a linear barotropic Rossby wave in the ocean interior which radiates energy offshore. Coastally trapped solutions occur when $k > k_c$. For this latter case the solutions are spatially damped as they propagate along the trench. Dispersion curves are presented for the coastally trapped solutions along the Japan, Kuril and Peru trenches. Surfaces of the mass transport streamfunction are also displayed for both evanescent and propagating solutions along the Japan, Kuril and Peru trenches. The theory suggests that leaky trench waves might be a generating mechanism for barotropic Rossby waves in the Pacific Ocean basin.

1. Introduction

Mysak *et al.* (1979) (hereafter denoted by MLE) show that oceanic trenches are a waveguide that can support two classes of barotropic, nondivergent topographic Rossby waves. Besides the familiar shelf waves which propagate their phase with shallow water to the right (left) in the Northern (Southern) Hemisphere, a set of "trench waves" also coexist and propagate their phase in the opposite direction to the former. Mysak and Willmott (1981) examined how the trench waves could be generated in the Japan–Kuril trench by the fluctuating transverse component of the Kuroshio as it flows eastward across the lower end of the trench, and in the Aleutian trench by the longshore component of the wind stress. Mysak and Willmott (1981) have shown that the shelf- and trench-wave eigenfunctions are mutually orthogonal and therefore the waves cannot interact. This allows the generation of either class of topographic Rossby waves that coexist on the trench to be considered independently. Mysak and Willmott (1981) also note that the long time scale associated with the trench wave modes will strongly couple motions over the trench to motions in the ocean interior via the β-effect. This paper studies the propagation of unforced trench waves along an ocean trench located on a midlatitude β-plane. The analysis of forced trench wave propagation on a β-plane is complicated. However, far from the generation zone, forced trench waves will perhaps propagate essentially as free waves and therefore have wave characteristics described in this study.

The governing equations for the model together with the appropriate matching and boundary conditions, are presented in Section 2. Solutions for freely propagating trench waves on a midlatitude β-plane are derived in Section 3. A long wave cutoff occurs for the existence of a trapped trench wave. Long waves which are not trapped radiate their energy into the ocean interior in the form of linear Rossby waves, thereby coupling dynamics over the trench with those in the ocean interior. Mysak (1978) noted that a similar long wave cutoff exists for trapped equatorial shelf waves on a flat continental shelf. In Section 4 dispersion curves and surfaces of the mass transport streamfunction associated with the trench waves propagating along trenches on both western and eastern sides of an ocean basin are presented.

2. Governing equations

A right-handed set of local Cartesian axes on a midlatitude β-plane is introduced, with the origin lying vertically above the deepest part of the trench ($x = 0$). Following MLE the x axis is directed away from the coast ($x = -L_1$), y along the coast and z upward. The trench is oriented so that the y axis is rotated clockwise through an angle ν from the north–south direction (see Fig. 1) With respect to these axes the Coriolis parameter takes the form

$$f = f_0 + \beta_c y - \beta_s x, \tag{2.1}$$

where

$$\beta_c = \beta \cos\nu, \quad \beta_s = \beta \sin\nu,$$

and f_0 is the value of the Coriolis parameter evaluated at the reference latitude (θ_0) of the β-plane and

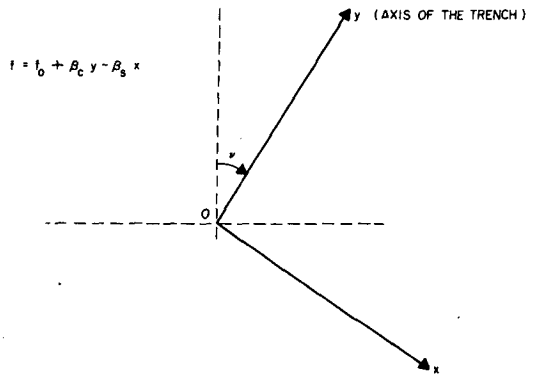

FIG. 1. Plan view of the coordinate system employed in the theory. The y axis lies over the deepest part of the trench.

$\beta = -2\Omega \cos(\theta_0)/R$ with Ω and R being the earth's angular velocity and radius.

The linearized equations for barotropic, nondivergent motions on a β-plane with depth profile $H(x)$ are given by

$$u_t - fv + \rho^{-1}p_x = 0, \tag{2.2}$$

$$v_t + fu + \rho^{-1}p_y = 0, \tag{2.3}$$

$$(Hu)_x + Hv_y = 0, \tag{2.4}$$

where u, v are the velocity components in the x, y directions, p is the pressure, ρ the density. In view of (2.4) it is convenient to introduce a mass transport streamfunction $\Psi(x, y, t)$ in which

$$Hu = -\Psi_y, \quad Hv = \Psi_x. \tag{2.5}$$

Substituting (2.5) into (2.2), (2.3) and eliminating p yields

$$\left(\frac{\Psi_x}{H}\right)_{xt} + \frac{\Psi_{yyt}}{H} + f\frac{H'}{H^2}\Psi_y + \beta_s\frac{\Psi_y}{H} + \beta_c\frac{\Psi_x}{H} = 0, \tag{2.6}$$

where the prime denotes differentiation with respect to x. The Coriolis parameter f in (2.6) assumes a constant value f_0. Plane wave solutions of (2.6) are sought, where Ψ takes the form

$$\Psi = \mathrm{Re}\{\psi(x)e^{i(ky-\omega t)}\}, \quad \omega > 0. \tag{2.7}$$

The amplitude function ψ then satisfies

$$\left(\frac{\psi'}{H}\right)' + \frac{i\beta_c}{\omega}\frac{\psi'}{H} - \frac{\beta_s k}{\omega}\frac{\psi}{H} - \frac{k^2}{H}\psi + f\frac{k}{\omega}\left(\frac{1}{H}\right)'\psi = 0. \tag{2.8}$$

In general, the solution for ψ will be complex. Furthermore, since wave-like solutions are required, the frequency ω is chosen to be a positive real number, and the wavenumber k is generally complex. Solutions of the form (2.7) will either be propagating waves or waves which are spatially damped.

Veronis (1966) discusses in detail how complex wavenumbers arise in (2.8) when assuming a plane wave solution for Ψ of the form (2.7). Because f is treated as a constant in (2.6), the term $i\beta_c\psi'/(\omega H)$ appears in (2.8), and this in turn leads to complex wavenumber solutions for real ω. If, however, the complete form of f is retained in (2.6) ($f = f_0 + \beta y$) it is not appropriate to seek solutions of the form (2.7). Although Veronis (1966) outlines how to proceed with the analysis of (2.6) when $f = f_0 + \beta y$, the method is not applicable to the rather complicated shelf/trench profile used in this study. Nevertheless it is useful to proceed with the solution of (2.8) for complex k when ω is assumed to be real because as Veronis (1966, p. 248) notes:

> . . . even though inconsistent results have been obtained by keeping f constant in the model, which combines β and bottom topography, the method of solution may still be useful. For example, in the plane-wave system, if one takes ω to be real and solves for the spatial variation, the solutions may be accurate locally, with the error becoming serious only at large distances from the point considered.

Indeed the hyperbola in $(\omega - k_R)$ space that is found to separate the leaky wave regime from the trapped wave regime will be unaltered if $f = f_0 + \beta y$ in (2.6). Furthermore, the points at which the dispersion curves for the trapped modes intersect the hyperbola will also remain the same if spatial variations in f are included in (2.6). It should be noted that Willmott and Bird (1982) show that the inclusion of spatial variations in f are required in (2.6) when considering long period (typically 100 days), long wavelength trench waves.

Following MLE a typical trench system is modeled by

$$H(x) = \begin{cases} H_1 = H_0 e^{2\alpha x}, & -L_1 \leq x \leq 0 \\ H_2 = H_0 e^{-2\gamma x}, & 0 < x \leq L_2 \\ H_3 = H_0 e^{-2\gamma L_2}, & L_2 \leq x < \infty. \end{cases} \tag{2.9}$$

The trench profile described by (2.9) is shown schematically in Mysak and Willmott (1981). At the coast the condition of no normal transport yields the boundary condition

$$\psi = 0 \quad \text{at} \quad x = -L_1. \tag{2.10}$$

Solutions which are trapped against the coast require

$$\psi \to 0 \quad \text{as} \quad x \to \infty. \tag{2.11a}$$

This far-field condition cannot be satisfied by all solutions of the form (2.7) and the more general far-field condition is

$$\psi \text{ is bounded as } x \to \infty. \tag{2.11b}$$

Continuity of the normal transport Hu and the pressure p at $x = 0$, L_2 requires

$$[\psi] = 0 \quad \text{at} \quad x = 0, L_2, \tag{2.12}$$

$$[\psi'] = 0 \quad \text{at} \quad x = 0, L_2. \tag{2.13}$$

System (2.8) and (2.10)–(2.13) defines an eigenvalue problem, where k is the eigenvalue and ψ is the corresponding eigenfunction. It is worth noting however, that on a β-plane, Eq. (2.8) is not self-adjoint. Therefore the eigenfunctions ψ are not complete and cannot be used as a basis for calculating a forced wave response on a β-plane in the manner of Mysak and Willmott (1981).

3. Trench wave solution on a β-plane

The analysis of (2.8) and (2.11) in the ocean interior determines the propagation characteristics of solutions given by (2.7). In the ocean interior, $H_3' = 0$ and (2.8) reduces to

$$\psi_3'' + \frac{i\beta_c}{\omega}\psi_3' - \left(\frac{\beta_s k}{\omega} + k^2\right)\psi_3 = 0, \qquad L_2 \leqslant x < \infty. \tag{3.1}$$

In the Appendix it is shown that the solutions of (3.1) have two possible forms:

1) A solution which is oscillatory in x and therefore satisfies (2.11b). In this case the wave number k is also real and positive for a trench in the Northern Hemisphere and satisfies the inequality constraint

$$0 < k < k_c, \tag{3.2}$$

where $k_c = \beta(1 - \sin\nu)/2\omega$. It is clear from (3.2) that on an f-plane, $k_c = 0$, and this solution is not possible. Furthermore when $\nu = 0$ (which corresponds to a trench oriented in the north–south direction) the value of k_c is a maximum and the associated cutoff wavelength $\lambda_c = 2\pi/k_c$ is a minimum. Waves with a wavelength $\lambda > \lambda_c$ will be oscillatory in the ocean interior, and will be designated as "leaky" modes. Leaky modes clearly take the form of Rossby waves in the region $L_2 \leqslant x < \infty$, and are required to radiate energy offshore. The solution for ψ_3 which satisfies (2.12) at $x = L_2$ is found to be

$$\psi_3 = \psi_2(L_2)\exp\left[-i\left(\mu + \frac{\beta_c}{2\omega}\right)(x - L_2)\right], \qquad L_2 \leqslant x < \infty, \tag{3.3}$$

where μ is a real number given by $\mu = [\beta^2/4\omega^2 - (k + \beta_s/2\omega)^2]^{1/2}$.

2) A solution which is trapped against the coast and therefore satisfies (2.11a). In this case the solution for ψ_3 which satisfies (2.12) at $x = L_2$ is given by

$$\psi_3 = \psi_2(L_2)\exp\left[-\left(\lambda + \frac{i\beta_c}{2\omega}\right)(x - L_2)\right], \qquad L_2 \leqslant x < \infty, \tag{3.4}$$

where

$$\lambda = \left[\left(k + \frac{\beta_s}{2\omega}\right)^2 - \frac{\beta^2}{4\omega^2}\right]^{1/2}.$$

In the Appendix it is shown that (3.4) is valid for complex k, with $\mathrm{Re}(k) = k_R > k_c$. Also $\mathrm{Im}(k) = k_I > 0$ for a trench in the Northern Hemisphere to produce exponential decay (rather than growth) in y. Solutions of this type are therefore non-propagating in both x and y directions.

Over the shelf region ($-L_1 \leqslant x \leqslant 0$) the substitution of the depth profile H_1 given by (2.9) into (2.8) yields

$$\psi_1'' - \left(2\alpha - \frac{i\beta_c}{\omega}\right)\psi_1' - \left(\frac{2fk\alpha}{\omega} + k^2 + \frac{\beta_s k}{\omega}\right)\psi_1 = 0. \tag{3.5}$$

The equation for ψ_2 in the trench region $0 \leqslant x \leqslant L_2$ is obtained from (3.5) by replacing α by $-\gamma$. The function ψ which satisfies the above equations, the boundary condition (2.10) and the jump conditions (2.12), is given by

$$\psi_1 = \frac{1}{2}Ae^{-\alpha L_1}\{\exp[m_1(x + L_1)] - \exp[m_2(x + L_1)]\}, \qquad -L_1 \leqslant x \leqslant 0, \tag{3.6}$$

$$\psi_2 = \frac{1}{2}[A\sinh(mL_1) - iB][\exp(n_1 x) - \exp(n_2 x)] + \frac{1}{2}Ae^{-\alpha L_1}[\exp(m_1 L_1) - \exp(m_2 L_1)]\exp(n_2 x), \qquad 0 \leqslant x \leqslant L_2, \tag{3.7}$$

where

$$\left.\begin{matrix} m_1 \\ m_2 \end{matrix}\right\} = \alpha - \frac{i\beta_c}{2\omega} \pm \left[\left(k + \frac{\beta_s}{2\omega}\right)^2 - \frac{\beta^2}{4\omega^2} + \alpha^2 + \frac{2fk\alpha}{\omega} - \frac{i\alpha\beta_c}{\omega}\right]^{1/2}, \tag{3.8}$$

$$\left.\begin{matrix} n_1 \\ n_2 \end{matrix}\right\} = -\gamma - \frac{i\beta_c}{2\omega} \pm \left[\left(k + \frac{\beta_s}{2\omega}\right)^2 - \frac{\beta^2}{4\omega^2} + \gamma^2 - \frac{2fk\gamma}{\omega} + \frac{i\beta_c\gamma}{\omega}\right]^{1/2}, \tag{3.9}$$

$$m = \left(\frac{2fk\alpha}{\omega} + \alpha^2 + k^2\right)^{1/2}, \tag{3.10}$$

and A and B are arbitrary constants. In (3.7) the complex constant term $[A\sinh(mL_1) - iB]$ is chosen so that solutions (3.6) to (3.10) reduce to the f-plane solutions of MLE when $\beta = 0$.

Substitutions of (3.4), (3.6) and (3.7) into (2.13) yields two homogeneous equations for A and B. Upon setting the determinant of coefficients of these two

equations to zero, the following general dispersion relation for coastally trapped solutions on a β-plane is obtained:

$$(n_1 - n_2)\left(n_2 + \lambda + \frac{i\beta_c}{2\omega}\right)\exp(n_2L_2) \times [\exp(m_1L_1) - \exp(m_2L_1)] + [(m_1 - n_2)\exp(m_1L_1) - (m_2 - n_2)\exp(m_2L_1)] \times \left[\left(n_1 + \lambda + \frac{i\beta_c}{2\omega}\right)\exp(n_1L_2) - \left(n_2 + \lambda + \frac{i\beta_c}{2\omega}\right)\exp(n_2L_2)\right] = 0. \quad (3.11)$$

In the limit as $\beta \to 0$ (f-plane) the dispersion relation (3.11) reduces to the trench wave dispersion relation derived by MLE.

4. Dispersion curves and eigenfunctions for trench waves

Following MLE it is convenient to nondimensionalize the problem. The nondimensional geometric parameters a, g, and r are introduced where

$$a = \alpha L_1, \quad g = \gamma L_1, \quad r = L_2/L_1.$$

The depth profile (2.9) then takes the form

$$H(x') = \begin{cases} H_0e^{+2ax'}, & -1 \leq x' \leq 0 \\ H_0e^{-2gx'}, & 0 \leq x' \leq r \\ H_0e^{-2gr}, & r \leq x' < \infty, \end{cases} \quad (4.1)$$

where $x' = x/L_1$. Defining a nondimensional frequency, wavenumber and beta by

$$\sigma = \omega/f_0, \quad \kappa = kL_1, \quad \hat{\beta} = \beta L_1/f_0$$

allows the nondimensional form of the dispersion relation (3.11) to be written as

$$(N_1 - N_2)\left(N_2 + \Gamma + \frac{i\hat{\beta}_c}{2\sigma}\right)\exp(N_2r) \times [\exp(M_1) - \exp(M_2)] + [(M_1 - N_2)\exp(M_1) - (M_2 - N_2)\exp(M_2)]\left[\left(N_1 + \Gamma + \frac{i\hat{\beta}_c}{2\sigma}\right)\exp(N_1r) - \left(N_2 + \Gamma + \frac{i\hat{\beta}_c}{2\sigma}\right)\exp(N_2r)\right] = 0, \quad (4.2)$$

where

$$\left.\begin{matrix} M_1 \\ M_2 \end{matrix}\right\} = a - \frac{i\hat{\beta}_c}{2\sigma} \pm \left[\left(\kappa + \frac{\hat{\beta}_s}{2\sigma}\right)^2 - \frac{\hat{\beta}^2}{4\sigma^2} + a^2 + \frac{2\kappa a}{\sigma} - \frac{ia\hat{\beta}_c}{\sigma}\right]^{1/2}, \quad (4.3)$$

$$\left.\begin{matrix} N_1 \\ N_2 \end{matrix}\right\} = -g - \frac{i\hat{\beta}_c}{2\sigma} \pm \left[\left(\kappa + \frac{\hat{\beta}_s}{2\sigma}\right)^2 - \frac{\hat{\beta}^2}{4\sigma^2} + g^2 - \frac{2\kappa g}{\sigma} + \frac{ig\hat{\beta}_c}{\sigma}\right]^{1/2}, \quad (4.4)$$

$$\Gamma = \left[\left(\kappa + \frac{\hat{\beta}_s}{2\sigma}\right)^2 - \frac{\hat{\beta}^2}{4\sigma^2}\right]^{1/2}. \quad (4.5)$$

Eq. (4.2) represents an implicit form of the dispersion relation [$\kappa = \kappa(\sigma)$] with r, a and b as parameters. For fixed values of the latter, the complex solutions $\kappa^{(n)}(\sigma) = \kappa_R^{(n)}(\sigma) + i\kappa_I^{(n)}(\sigma)$, $n = 0, 1, 2, \cdots$ of (4.5) are calculated. In the Northern Hemisphere $\kappa_R^{(n)} > 0$ and $\kappa_I^{(n)} > 0$, $n = 0, 1, 2, \ldots$.

The nondimensional form of (3.3), (3.4), (3.6) and (3.7) is required. For a particular root $\kappa^{(n)}(\sigma)$, the corresponding nondimensional coastally trapped nth-mode trench wave eigenfunction can be written as

$$\psi^{(n)} = \begin{cases} \psi_1^{(n)} = \frac{1}{2}e^{-\alpha}\{\exp[M_1(x' + 1)] - \exp[M_2(x' + 1)]\}, & -1 \leq x' \leq 0 \\ \psi_2^{(n)} = \frac{1}{2}[\sinh(M) - iB][\exp(N_1x') - \exp(N_2x')] \\ \qquad + \frac{1}{2}e^{-\alpha}[\exp(M_1) - \exp(M_2)]\exp(N_2x'), & 0 \leq x' \leq r \\ \psi_3^{(n)} = \psi_2^{(n)}(r)\exp\left[-\left(\Gamma + \frac{i\hat{\beta}_c}{2\sigma}\right)(x' - r)\right], & r \leq x' < \infty, \end{cases} \quad (4.6)$$

where

$$A = 1, \quad M = \left[\frac{2a\kappa}{\sigma} + a^2 + \kappa^2\right]^{1/2},$$

$$B = \{e^{-\alpha}[(M_1 - N_2)\exp(M_1) - (M_2 - N_2)\exp(M_2)] - (N_1 - N_2)\sinh(M)\}/(N_2 - N_1).$$

The nondimensional counterpart of the dimensional leaky trench wave eigenfunction (3.3) is given by

$$\psi_3 = \psi_2(r)\exp\left[-i\left(\Pi + \frac{\hat{\beta}_c}{2\sigma}\right)(x' - r)\right], \quad r \leq x' \leq \infty, \quad (4.7)$$

where

$$\Pi = \left[\frac{\hat{\beta}^2}{4\sigma^2} - \left(\kappa + \frac{\hat{\beta}_s}{2\sigma}\right)^2\right]^{1/2},$$

$$0 \leq \kappa \leq \frac{\hat{\beta}}{2\sigma}(1 - \sin\nu).$$

For the Japan, Kuril, and Peru trenches, dispersion curves are plotted in $(\sigma - \kappa_R)$ and $(\sigma - \kappa_I)$ space by solving the dispersion relation (4.2) associated with trapped solutions. Leaky modes do not have a quantized wavenumber because they exist in the semi-infinite region $x > -L_1$. In $(\sigma - \kappa_R)$ space the continuum of leaky modes occupies the region bounded by the hyperbola $\sigma = \hat{\beta}(1 - \sin\nu)/(2\kappa)$ and the coordinate axes in the first quadrant. For trenches that are more zonally aligned ($\nu \to \pi/2$) this region becomes smaller, and in the limit vanishes when $\nu = \pi/2$.

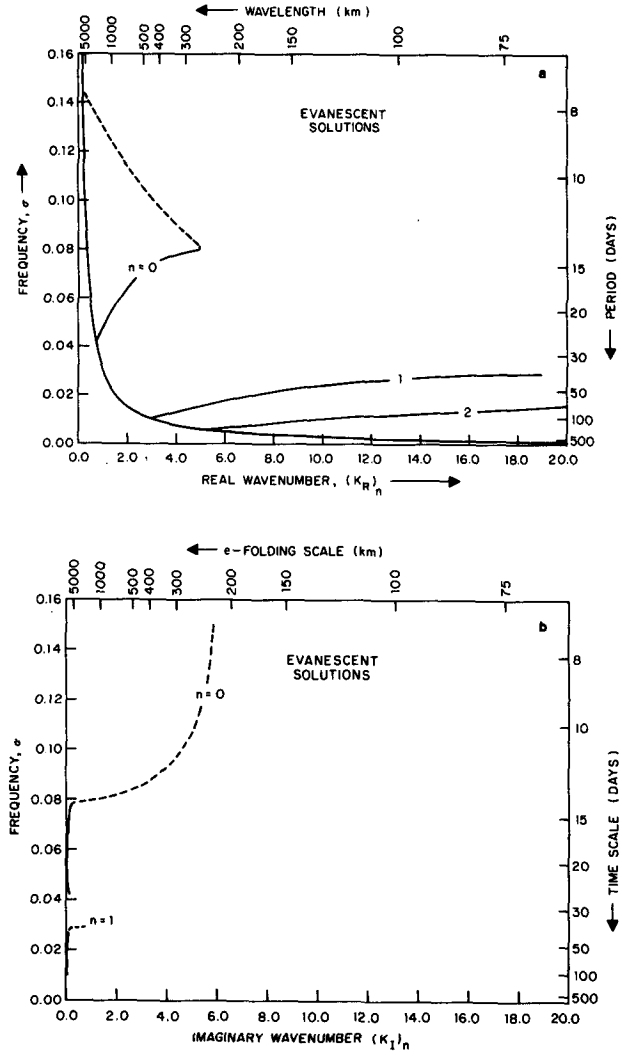

FIG. 2. Dispersion curves for the Japan trench when $\nu = 0$ is plotted in (a) σ-κ_R space, and (b) σ-κ_I space. The values $L_1 = 208$ km and $f = 0.662 \times 10^{-4}$ s^{-1} (corresponding to latitude 27°N) are used to calculate the wavelengths and periods, respectively. The dashed lines correspond to strongly damped solutions. In the region bounded by the hyperbola and the coordinate axes, a continuum of propagating wave solutions exists.

TABLE 1. Values of the critical period and critical wavelength at the points where the dispersion curves in $(\sigma - \kappa_R)$ space intersect the hyperbola $\sigma_c = \hat{\beta}(1 - \sin\gamma)/2\kappa_c$ for the Japan, Kuril and Peru trenches.

Trench	Mode number (n)	Critical period (days)	Critical wavelength (km)
Japan	0	26.28	1706.0
	1	102.00	440.3
	2	180.10	255.0
Kuril	0	29.8	6394.0
	1	120.8	1522.0
	2	310.5	620.0
Peru	0	46.68	876.2
	1	157.00	261.1
	2	268.63	150.92

Figure 2 shows the dispersion curves in $(\sigma - \kappa_R)$ and $(\sigma - \kappa_I)$ space for the Japan trench with $\nu = 0$. The origin of the coordinate system is located at 27°N and the parameter values used to fit the trench are given in MLE. To the right of the hyperbola in Fig. 2a the dispersion curves are associated with evanescent solutions of two distinct types. For each of the first three modes displayed in Fig. 2a, the solid dispersion curve represents solutions which are essentially undamped. In $(\sigma - \kappa_I)$ space shown in Fig. 2b the values of κ_I corresponding to the frequency range spanned by the solid dispersion curves in Fig. 2a are small. As expected, the dispersion properties of the lightly damped solutions are almost identical to the dispersion properties of the trench waves examined by MLE. The dashed lines in Fig. 2 represent solutions which are strongly damped spatially and exist only for sufficiently long wavelengths. For each mode, the latter solutions exist provided that $\kappa_c < \kappa < \kappa_s$, where κ_s is the wavenumber value where the slope of the dispersion curve in $(\sigma - \kappa_R)$ space vanishes.

The critical period and wavelength at the point where the dispersion curves corresponding to the solid lines intersect the hyperbola, for the first three modes along the Japan trench, are given in Table 1. Also presented in Table 1 are the corresponding points for the Kuril and Peru trenches. These points are of particular interest because they mark the transition point between propagating and evanescent solutions for each mode. Along the dispersion curves denoted by a solid line in Figs. 2a and 3a, the group velocity c_g of the weakly damped waves is in the same direction as the phase speed. However, along the dispersion curves denoted by a dashed line, the spatial damping of the waves is much larger and the group velocity

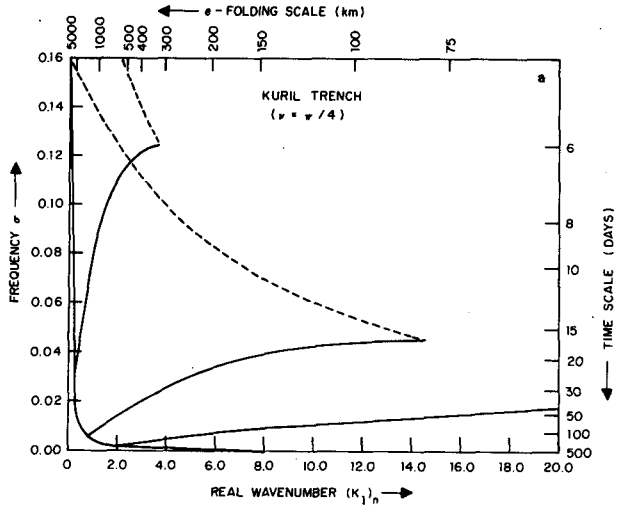

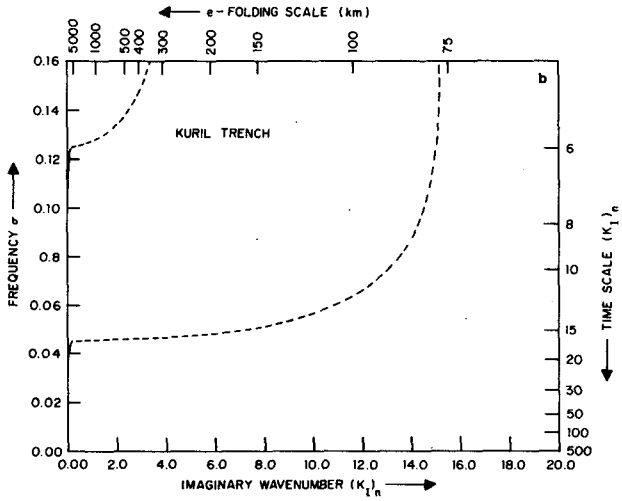

FIG. 3. As in Fig. 2, except the Kuril trench parameters are used. For this case $\nu = 45°$, $L_1 = 185$ km and $f = 0.976 \times 10^{-4}$ s^{-1} (corresponding to latitude 42°N).

of the solutions is negative. Therefore energy propagation by the evanescent solutions will mostly occur in the northward direction in the Japan trench.

Fig. 3 shows the dispersion curves for the Kuril trench. For this trench, the parameters appearing in (2.9) are given in MLE and the origin of the coordinate system is located at 42°N with the y axis rotated 45° clockwise from the north–south direction. Propagating solutions are confined to a smaller region of $(\sigma - \kappa_R)$ space than in the previous case. The evanescent solutions corresponding to the broken line dispersion curves are seen to exhibit larger spatial decay than in the Japan trench. Therefore, southward energy propagation in the Kuril trench will be terminated more rapidly than in the Japan trench.

Fig. 4 shows the dispersion properties of free waves for the Peru trench when the origin of the coordinate system is located at 10°S. Unlike the previous two cases, $\kappa_I < 0$ to ensure that the solutions spatially decay in the negative y direction (towards the equator). The axis of the trench is oriented north–south.

To show the structure of the free waves across the shelf, trench and abyssal plane, the surface generated by the mass transport streamfunction $\Psi(x, 0, t)$ is plotted for the Japan and Peru trenches. Figures 5 and 6 show the plot of the surface generated by $\Psi(x, 0, t)$ for the first three weakly damped modes along the Japan and Peru trenches, respectively. The evanescent nth mode exhibits $(n + 1)$ turning points across the trench. Furthermore the largest amplitude of $\Psi(x, 0, t)$ occurs over the trench. Figure 7a displays a leaky mode along the Japan trench and clearly

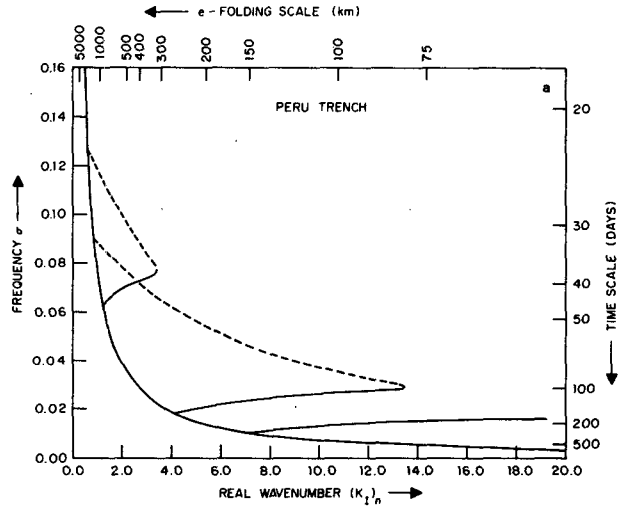

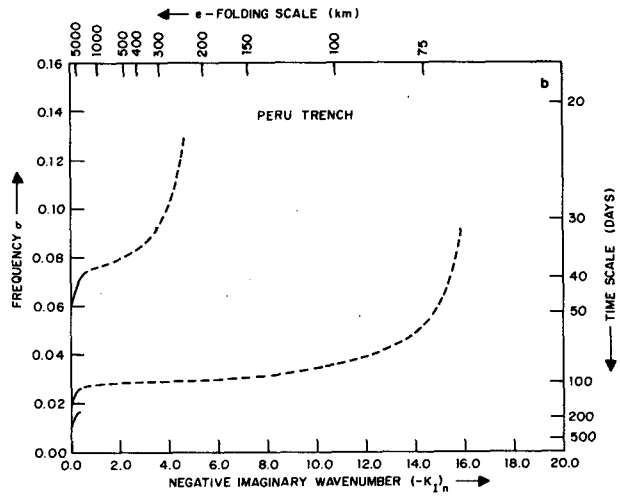

FIG. 4. As in Fig. 2, except the Peru trench parameters are used. For this case, $\nu = 180°$, $L_1 = 171$ km and $f = -0.253 \times 10^{-4}$ s^{-1} (corresponding to latitude 10°S).

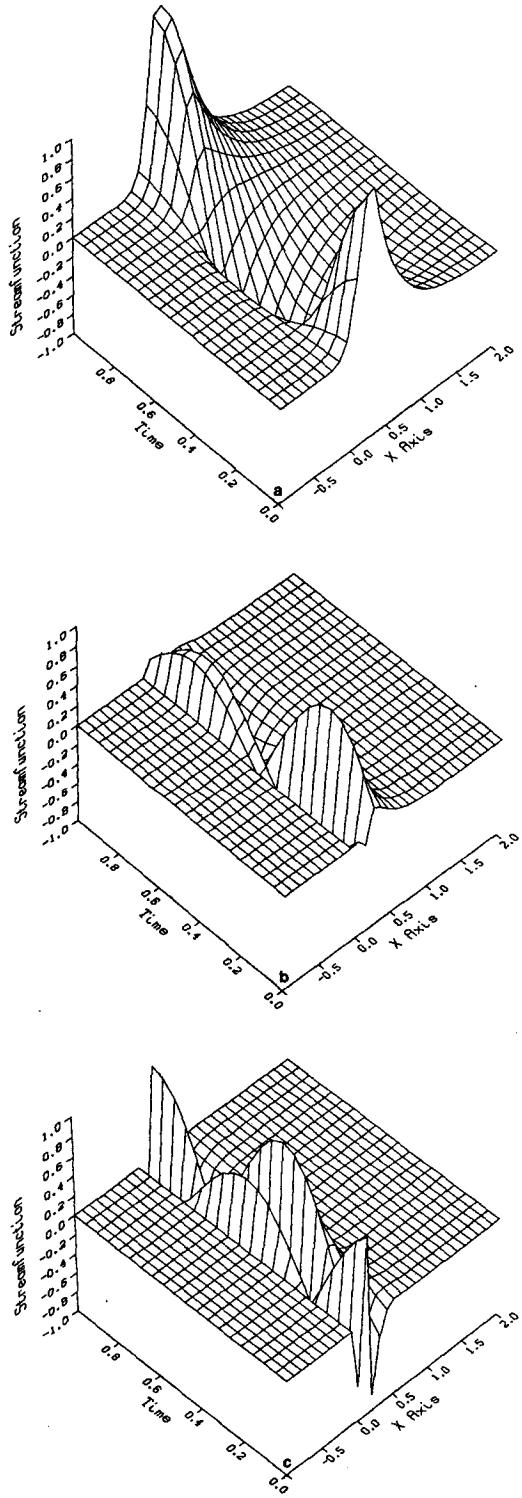

FIG. 5. Plot of the surface generated by the mass transport streamfunction $\Psi(x, 0, t)$ for the lightly damped evanescent solutions in the Japan trench. The values of σ chosen for the three modes (a) $n = 0$, (b) $n = 1$ and (c) $n = 2$ are 0.07, 0.02 and 0.01, respectively. The amplitude of Ψ is normalized for modes $n = 0$, 1 and 2 by multiplying by the factors 10^{-5}, 10^{-16}, and 10^{-26}, respectively.

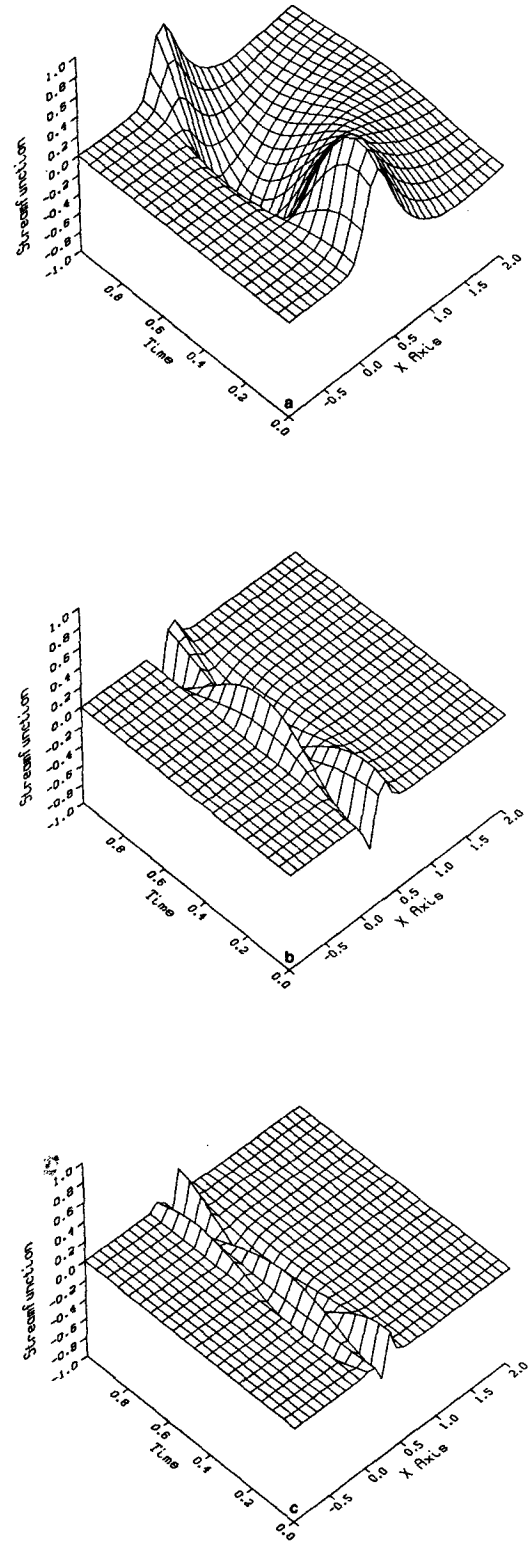

FIG. 6. As in Fig. 5, for the Peru trench, except the values of σ chosen for the modes (a) $n = 0$, (b) $n = 1$, and n = (c) $n = 2$ are 0.07, 0.025, and 0.015 and the amplitude of Ψ is normalized for modes $n = 0$, 1 and 2 and by multiplying by the factors 10^{-5}, 10^{-17} and 10^{-28}, respectively.

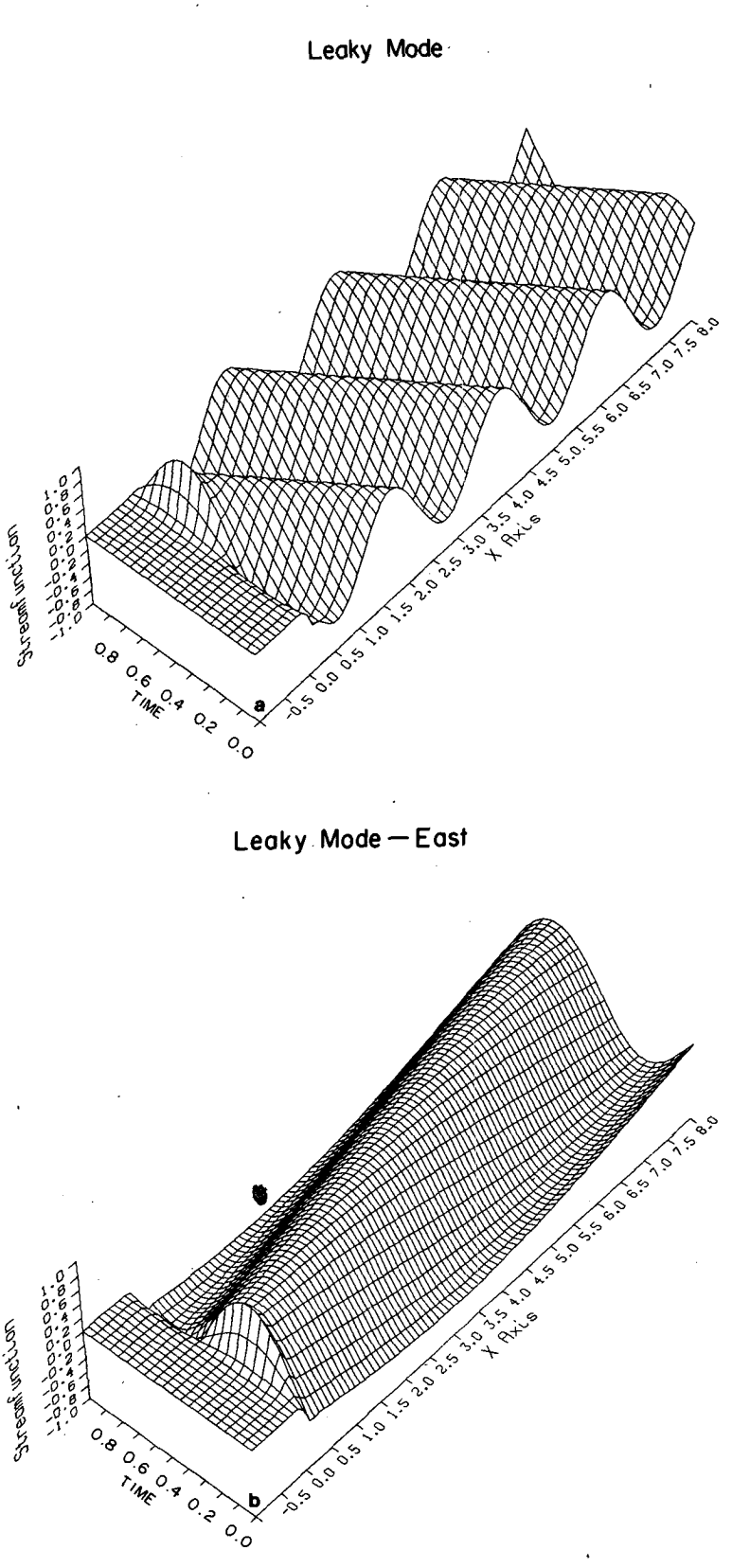

FIG. 7. Plot of the surface generated by the mass transport streamfunction $\Psi(x, 0, t)$ for a propagating solution along the Japan trench when the trench is located (a) on the western side of the ocean basin ($\nu = 0$) and (b) on the eastern side of the ocean basin ($\nu = \pi$). The parameter values $\kappa = 1.0$ and $\sigma = 0.02$ are chosen and the wavelength of the Rossby wave in the ocean interior is calculated to be (a) 458.1 km and (b) 3728.2 km. The amplitude of Ψ is normalized for both (a) and (b) by multiplying with the factor 10^{-6}.

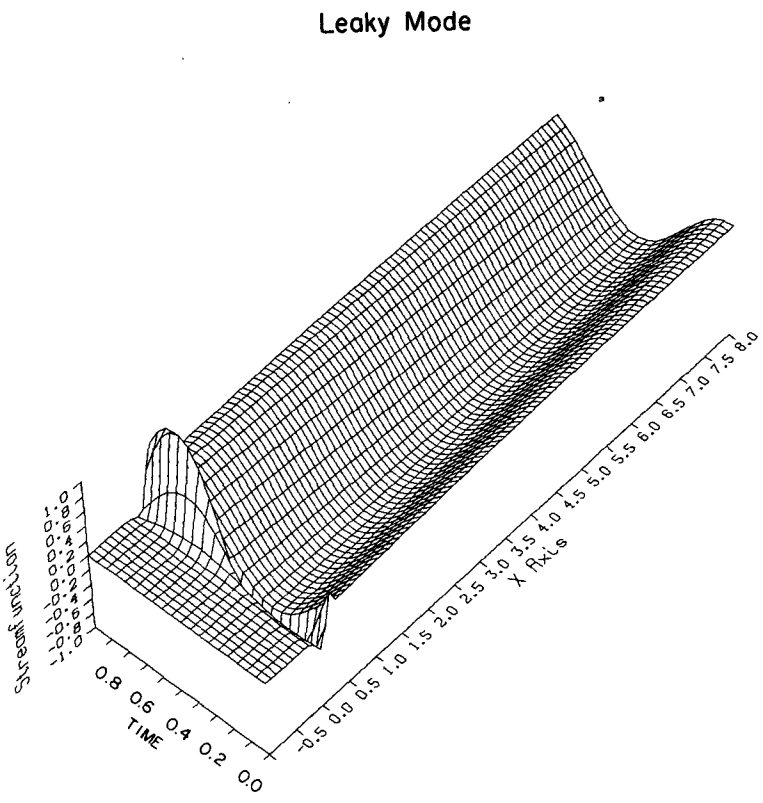

FIG. 8. Plot of the surface generated by the mass transport streamfunction $\Psi(x, 0, t)$ for a propagating solution along the Peru trench with $\nu = \pi$. The parameter values $\kappa = 1.0$ and $\sigma = 0.02$ are chosen and the amplitude of Ψ is normalized by multiplying by the factor 10^{-6}.

shows linear Rossby wave propagation in the ocean interior. In Fig. 7b, the corresponding leaky mode is displayed when the Japan trench is translated to the eastern side of the North Pacific (where $\nu = \pi$). As expected the offshore wavelength of the Rossby waves is longer than in Fig. 7a. A leaky trench wave mode for the Peru trench is also displayed in Fig. 8. The excitation of leaky trench waves along major Pacific Ocean trenches might lead to another source of Rossby wave activity in the ocean interior. However, in the North Pacific recent studies (see Kang and Magaard, 1980; White and Saur, 1981) show that baroclinic rather than barotropic Rossby waves are observed. The inclusion of stratification in this calculation will produce a more realistic Rossby wave field in the ocean interior. The difficulties in doing this are that the stratification in deep trenches is likely to be different from that over the ocean interior, and therefore a matching problem for the waves in differently stratified regions will arise. Brink (1983) has examined the effect of stratification on freely propagating trench waves on an f-plane. The model developed by Brink (1983) is continuously stratified, but the dynamics over the trench are decoupled from those in the ocean interior because of the f-plane assumption. Nevertheless, Brink (1983) shows that stratification can substantially alter the phase speed magnitude of each mode and give rise to bottom intensified currents.

5. Conclusions

This study shows that including variations of the Coriolis parameter with latitude substantially alters the free wave characteristics of trench waves. Trench waves with a wavelength greater than a critical wavelength are not coastally trapped. Over the ocean interior the leaky modes take the form of linear barotropic Rossby waves. Trench waves with wavelength less than the critical wavelength exhibit spatial decay as they propagate along the trench. The evanescent solutions fall into two classes:

1) Weakly damped solutions which have dispersion properties similar to MLE.
2) Strongly damped solutions with group velocity directed opposite to the phase velocity of trench waves.

Solutions of type 2 only occur at longer wavelengths where the variation of the Coriolis parameter with latitude is likely to be felt.

Acknowledgments. This work was supported by the NPS Foundation Research Program. Additional financial support is also provided by the U.S. Office

of Naval Research, Code 422(PO). The authors thank Lawrence Mysak for helpful discussions.

APPENDIX

Solution of the Amplitude Function ψ_3 in the Ocean Interior

It is convenient when solving (3.1) to make a change of dependent variable by writing

$$\psi_3 = \exp(-i\beta_c x/2\omega)\phi,$$

whence ϕ satisfies

$$\phi'' + \mu^2\phi = 0, \tag{A1a}$$

where

$$\mu^2 = \frac{\beta^2}{4\omega^2} - \left(k + \frac{\beta_s}{2\omega}\right)^2. \tag{A1b}$$

The general solution of (A1) requires $\omega \in \mathcal{R}$ and k to be a complex number of the form $k = k_R + ik_I$, where k_R, $k_I > 0$. Therefore the general solution of (A1) can be written as

$$\phi = Ae^{\mu_I x}e^{i\mu_R x} + Be^{-\mu_I x}e^{-i\mu_R x}, \tag{A2}$$

where

$$\left.\begin{aligned} \mu_R &= R^{1/2}\cos\frac{\theta}{2}, \qquad \mu_I = R^{1/2}\sin\frac{\theta}{2} \\ R^2 &= P^2 + Q^2 \qquad \tan\theta = \frac{Q}{R} \end{aligned}\right\},$$

with

$$\left.\begin{aligned} P &= \frac{\beta^2}{4\omega^2} - \left(k_R + \frac{\beta_s}{2\omega}\right) + k_I^2 \\ Q &= 2k_I\left(k_R + \frac{\beta_s}{2\omega}\right) \end{aligned}\right\}.$$

It is permissible for (A2) to be purely oscillatory in x by requiring $\mu_I = 0$. In this case

$$\sin\frac{\theta}{2} = 0,$$

which leads to the condition that

$$Q = 2k_I\left(k_R + \frac{\beta_s}{2\omega}\right) = 0. \tag{A3}$$

Since $k_R > 0$, the required solution of (A3) is $k_I = 0$, which says that solutions which are not coastally trapped (leaky solution) must have real wavenumbers. Furthermore, the leaky solutions require

$$0 < k < k_c = \beta(1 - \sin\nu)/2\omega.$$

For the leaky wave solution, (A2) can now be written as

$$\phi = Ae^{i\mu x} + Be^{-i\mu x}, \tag{A4}$$

where

$$\mu = \left[\frac{\beta^2}{4\omega^2} - \left(k_R + \frac{\beta_s}{2\omega}\right)^2\right]^{1/2}.$$

Clearly one of the terms on the rhs of (A4) must be unacceptable on physical grounds. To see this, the time dependence is reintroduced in the leaky wave solution (A4), yielding

$$\psi_3 e^{-i\omega t} = A\exp\left\{i\left[\left(\mu - \frac{\beta_c}{2\omega}\right)x - \omega t\right]\right\}$$

Term I

$$+ B\exp\left\{i\left[-\left(\mu + \frac{\beta_c}{2\omega}\right)x - \omega t\right]\right\}. \tag{A5}$$

Term II

Solution (A5) exhibits the propagation characteristics in the x-direction of the Rossby wave in the ocean interior ($x > L_2$). Let k_1 and k_2 be the effective wavenumbers in the x-direction of Terms I and II respectively in (A5). Then

$$k_1 = \mu - \frac{\beta_c}{2\omega}, \quad k_2 = \mu + \frac{\beta_c}{2\omega}.$$

At an eastern boundary aligned in the north–south direction ($\nu = \pi$), $k_1 > k_2$. Term II in (A5) is therefore associated with long waves propagating from this boundary. Similarly at a western boundary aligned north–south ($\nu = 0$) $k_1 < k_2$, which therefore implies Term II is associated with the short wave propagation from this boundary. Term I is rejected therefore, in the leaky wave solution and consideration of the slowness curves for the resulting Rossby wave solution shows that energy propagation is directed offshore.

For solutions that are coastally trapped, the first term on the rhs of (A2) must be rejected, and the resulting solution for ϕ can be written as

$$\phi = Be^{-\lambda x},$$

where

$$\left.\begin{aligned} \lambda &= \left[\left(k + \frac{\beta_s}{2\omega}\right)^2 - \frac{\beta^2}{4\omega^2}\right]^{1/2} \\ &\mathrm{Re}(k) > k_c \end{aligned}\right\}.$$

REFERENCES

Brink, K. H., 1983: Some effects of stratification on long trench waves. *J. Phys. Oceanogr.*, **13**, 496–500.

Kang, Y. Q., and L. Magaard, 1980: Annual baroclinic Rossby waves in the central North Pacific. *J. Phys. Oceanogr.*, **10**, 1159–1167.

Mysak, L. A., 1978: Long-period equatorial topographic waves. *J. Phys. Oceanogr.*, **8**, 302–314.

——, and A. J. Willmott, 1981: Forced trench waves. *J. Phys. Oceanogr.*, **11**, 1481–1502.

——, P. H. LeBlond and W. J. Emery, 1979: Trench waves. *J. Phys. Oceanogr.*, **9**, 1001–1013.

Veronis, G., 1966: Rossby waves with bottom topography. *J. Mar. Res.*, **24**, 338–349.

White, W. B., and J. F. T. Saur, 1981: A source of annual baroclinic waves in the eastern subtropical North Pacific. *J. Phys. Oceanogr.*, **11**, 1452–1462.

Willmott, A. J., and A. A. Bird, 1982: Freely propagating trench waves on a beta-plane. Ocean modeling. (unpublished manuscript)